

## *In situ* resistance measurements of YBaCuO thin films during the oxygenation process for various elaboration conditions

F. Hosseini Teherani\*, E. Caristan, J.M. Depond, T. Pech, F. Carrié and A. Kreisler

Laboratoire de Génie Electrique de Paris (LGEF) - Universités Paris 6 et Paris 11 - URA n°127 du CNRS  
SUPELEC - Plateau de Moulon, 91192 GIF SUR YVETTE CEDEX, FRANCE

### Abstract

For YBaCuO films sputtered on polycrystalline YSZ, resistance monitoring during various oxygenation processes is reported. *Ex situ* rapid thermal annealing is considered first and compared with regular long annealing. A common feature is a temporary liquid phase state from which the superconducting material nucleates. *In situ* elaboration is then commented, while stressing upon possible parasitic superionic conductivity of the substrate.

### 1. Introduction

Following early *in situ* electrical characterizations of low temperature sputtered YBaCuO thin films during a rapid thermal annealing (RTA) process [1], we have performed further resistance measurements to optimize the film properties with respect to elaboration conditions. We have considered *ex situ* techniques, where nucleation, grain growth and oxygenation are performed either by RTA or by a long thermal anneal (LTA) posterior to low temperature (i.e. amorphous) film sputtering, and studied the high temperature (600–800 °C) *in situ* sputtering technique as well.

In view of device development such as current switches or limiters [2], or radiation detectors [3], yttria stabilized polycrystalline zirconia substrates (YSZ) with 8 mol %  $Y_2O_3$  were used [4]. Whereas this choice was dictated by economical considerations for the former application, the low thermal conductivity was a selection criterion for the latter. When considering electrical measurements at high temperatures with these substrates, special interest had to be taken to account for their superionic properties [5].

Resistance monitoring during *in situ* elaboration helps to understand the oxygen exchange between the substrate and the film and so to adjust its oxygen content.

### 2. Experimental procedures

#### 2.1. Electrical characterizations during *ex situ* annealing

The elaboration procedure of amorphous YBaCuO films by low temperature (<400°C) rf diode sputtering on polycrystalline YSZ (with 3 or 8 mol %  $Y_2O_3$ ) has been detailed elsewhere [2]. After deposition, the insulating films were treated either by RTA or LTA.

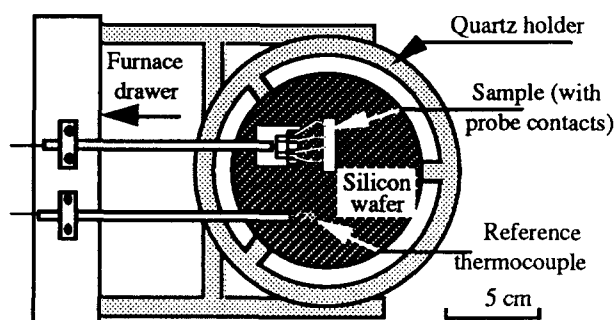


Figure 1. Sketch of the electrical characterization inside the RTA furnace (ADDAX # R1000, Grenoble, France)

A typical RTA cycle included a (10 s) heating up phase and a (60 s) high temperature dwell at  $T_{max}$  (measured by a reference thermocouple, figure 1) under flowing argon, followed by cooling down under flowing oxygen (for about 5 min.). The RTA furnace made use of 12 high power incandescent lamps, allowing the sample (which was placed on a silicon substrate wafer inside a quartz enclosure) to reach 1000°C within 3 seconds [6].

Considering the heating process, the electrical contacts in view of high temperature four-probe resistivity measurements had to be made as small as possible, so that no shadowing affected the radiation absorption by the material. Furthermore, the size of the potential probes had to be similar, so that the cooling of the material through the probes was symmetrical. By this way, we could neglect thermocouple effects during the measurements. The contacts (6 mm spaced) were realized by using 50  $\mu$ m diameter gold wires directly thermal-bonded onto the YBaCuO film. The system used for the high temperature four-probe resistance measurements is represented in figure 1. These were controlled by a desktop calculator at a rate of one measurement point every 0.18 s.

The LTA cycle consisted of a ( $\leq 180$  min.) heating step followed by a (15 min.) dwell at  $T_{max}$  under flowing argon, and cooling down under oxygen. After having

\* Present address: NTT Interdisciplinary Research Laboratories, 162 Tokai, Ibaraki 319-11, Japan

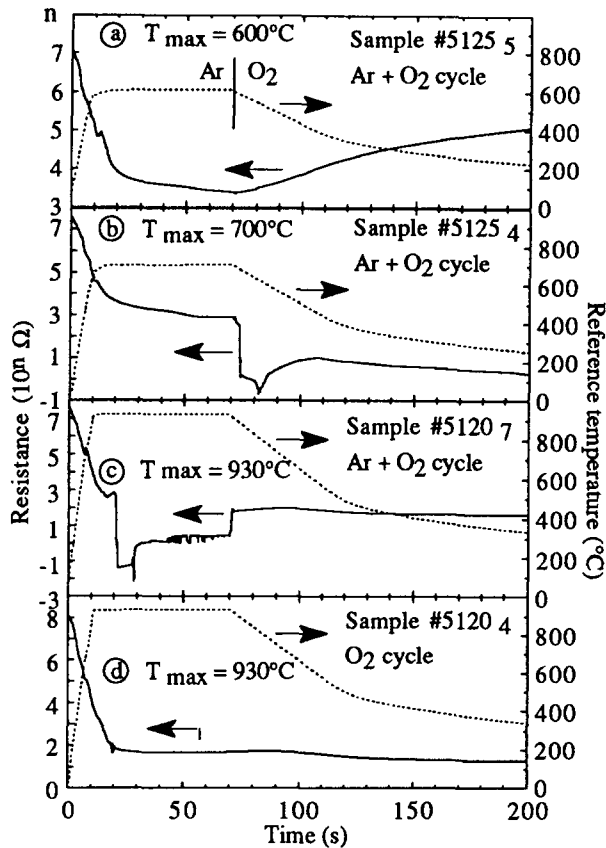


Figure 2. Sample resistance and temperature variations during RTA annealing (samples of nearly identical dimensions)

reached 500°C and maintained this temperature for a (0 to 1 h duration) optional dwell, the final cooling down to room temperature has been achieved under inertial conditions. The measuring arrangement is similar to that used for the RTA, however with a lower (15 s) sampling rate.

## 2.2. In situ elaboration and substrate characterizations

*In situ* elaboration of YBaCuO films was performed by rf planar magnetron sputtering with an Ar + O<sub>2</sub> mixture at  $T_{\max}$  = 600 to 800°C substrate temperature (measured with a thermocouple placed onto the sample surface), followed by an oxygenation phase at  $T_{\max}$  and during cooling down. In order to monitor the film resistance during this phase, electrical contacts had to be made onto the substrate prior to sputtering. This was accomplished by ultrasonically bonding gold wires to narrow conducting multilayer strips shadow mask sputtered (1st layer: YBaCuO) and sequentially evaporated under vacuum (2nd and 3rd layers: Ag and Au, respectively). This technique was also very helpful to test the electrical behaviour of bare substrates during various heating cycles.

## 3. Ex situ thermal annealing (RTA or LTA)

### 3.1. Influence of $T_{\max}$

Our main results concerning the value of  $T_{\max}$  and the

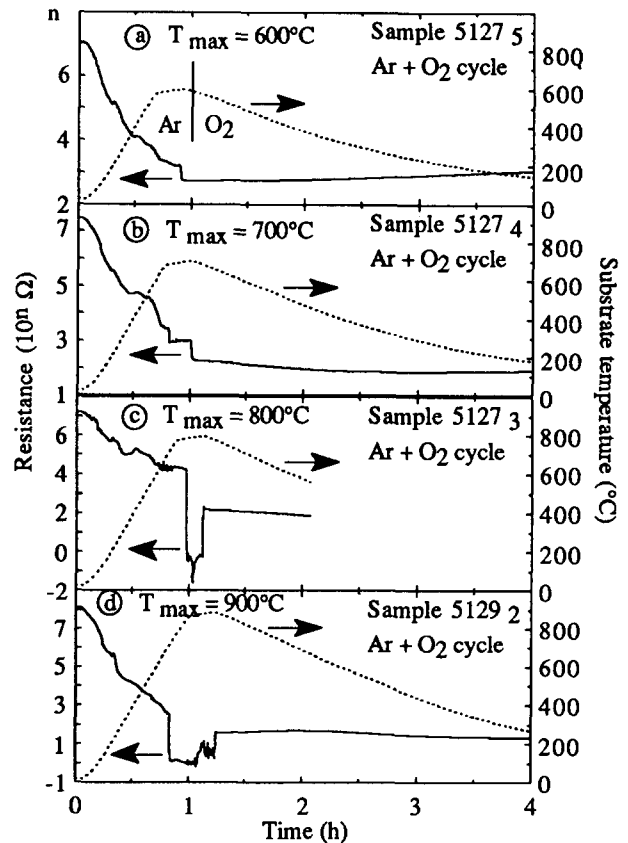


Figure 3. Sample resistance and temperature variations during LTA annealing (samples of nearly identical dimensions)

annealing atmosphere during the RTA are summarized in Fig. 2, which shows the film resistance variation for several films sputtered at 375°C during similar runs (film thickness about 9000 Å, width 3 mm, and Y:Ba:Cu composition 1:2.2:3.3).

For an annealing cycle as described in section 2.1., the prominent conclusions relative to  $T_{\max}$  are: i) For  $T_{\max} \leq 600^\circ\text{C}$ , the resistance variations reveal no noticeable crystallization; in fact, the film surface was shiny after RTA and no grains could be observed by optical microscopy. ii) For  $600 < T_{\max} \leq 900^\circ\text{C}$ , the resistance drops significantly when O<sub>2</sub> is introduced; this behaviour is attributed to the tetragonal-orthorhombic (T-O) i.e. semiconductor-metallic transition of the YBaCuO grains. The latter appear during the dwell under Ar and grow with the tetragonal structure, the oxygen content being low under these conditions. iii) For  $T_{\max} \geq 930^\circ\text{C}$ , the resistance drops drastically during the dwell and, in contrast with case ii), the resistance increases when oxygen is introduced. Moreover, we observe large grains such as needles after annealing. This unusual resistance behaviour can be attributed to a liquid-solid transformation, as reported by Lindemer et al. [7] whose (T-pO<sub>2</sub>) phase diagram indicates that at 930°C under argon, a liquid (1-2-3) phase and the green (2-1-1) phase should be present, whereas solidification should occur rapidly when argon is replaced by oxygen.

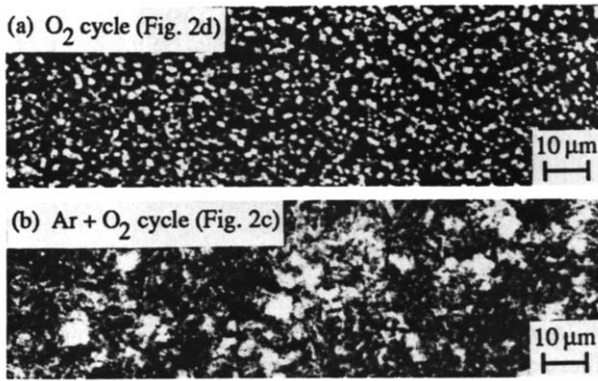
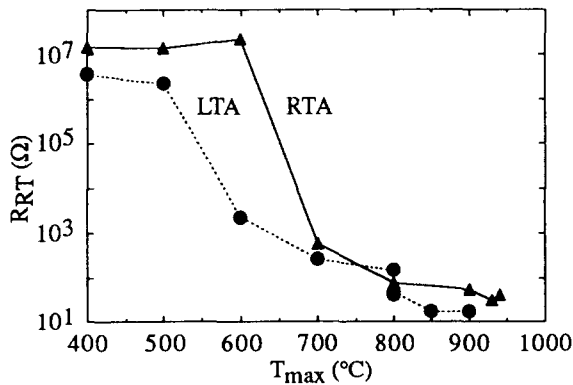


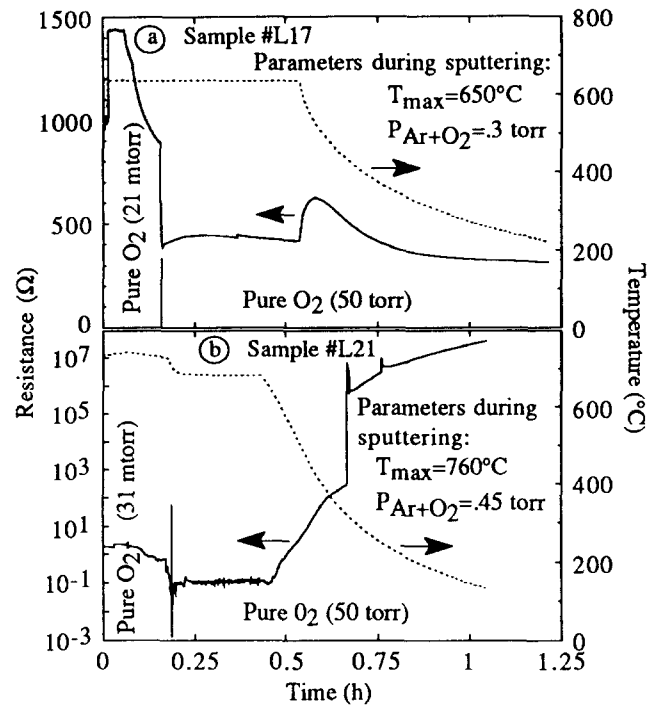
Figure 4. Optical micrographs of YBaCuO films after RTA

Figure 5.  $R_{RT}$  room temperature resistance of the YBaCuO thin films versus  $T_{max}$  annealing temperature

A similar behaviour of the film resistance was observed during LTA, as shown in figure 3 for various values of  $T_{max}$ . Again, for sufficiently large values of  $T_{max}$  (typically above 800°C), a sharp resistance drop is observed in the dwell region, which is also attributed to the temporary presence of a high conductivity liquid phase. Such phase transformations concern the surface and the bulk of the film. However, two other phenomena should also be considered at the film/substrate interface: the interdiffusion of Zr and Ba (which changes the composition), and the oxygen outdiffusion from YSZ. Moreover, the resistance drop during the dwell might also be attributed to percolation phenomena at the interface [8]; this latter point is considered in section 4.

### 3.2. Influence of the annealing atmosphere

The influence of the gas nature during the annealing process is demonstrated by comparing figures 2 (c) and (d), the latter being relative to the whole RTA cycle performed under oxygen. Films obtained by this latter treatment consisted of small grains (Fig. 4a) with no preferential orientation, whereas those heated under argon were textured along the YBaCuO *c*-axis [4], with large grains (Fig. 4b). The difference in resistance behaviour confirms that increasing the  $O_2$  content during annealing increases the melting point of both YBaCuO and impurity phases [9].

Figure 6. Sample resistance and temperature behaviour during *in situ* film elaboration (after rf magnetron sputtering )

### 3.3. Thin film electrical characteristics

The room temperature resistance  $R_{RT}$  of the studied samples versus  $T_{max}$  for both RTA and LTA anneals offer striking similarities (figure 5). The excessively high values obtained for  $T_{max} \leq 600^\circ\text{C}$  clearly suggest that crystallisation of YBaCuO is significant only for  $T_{max} \geq 700^\circ\text{C}$ . In fact, it was shown in [7] that the formation of the YBaCuO solid compound should occur under argon annealing at 700 °C.

However, no crystalline structure was visible by optical microscopy and a semiconductor-like behaviour of the resistance was observed at low temperatures for  $700^\circ\text{C} < T_{max} < 900^\circ\text{C}$ . This result might be explained by the crystalline phase being embedded into amorphous phases.

## 4. *In situ* elaboration and substrate behaviour

### 4.1. General considerations

In order to help optimizing the sputtering and oxygenation parameters during *in situ* elaboration of YBaCuO films on polycrystalline YSZ substrates, the resistance of the samples was monitored (see section 2.2. for details), as already reported by other authors [9]. The main parameters are the argon and oxygen partial pressures and substrate temperature during sputtering (during which the film resistance cannot be measured due to electric discharge interference), as well as the oxygen pressure and temperature profile posterior to the sputtering phase. Two extreme cases are shown in figure 6. Sample L17 corresponds to nearly optimized sputtering conditions,

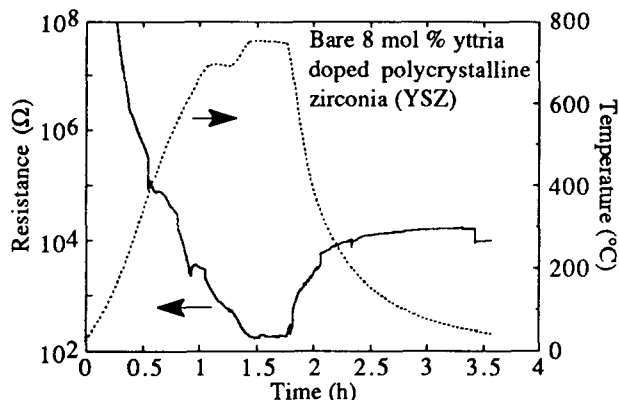


Figure 7. YSZ substrate resistance and temperature behaviour during a thermal cycle performed under vacuum

accompanied by a sharp resistance drop as oxygen is introduced into the reaction chamber (T-O transformation) and subsequent metallic behaviour during cooling down. In contrast, sample L21 corresponds to not optimized sputtering conditions (too high argon pressure and too high substrate temperature), with the consequence of a semiconducting behaviour during the oxygenation phase.

We have to stress that extreme care should be taken while interpreting these plots. In fact, the high temperature resistance data are strongly influenced by the very large ionic conductivity values characterizing the YSZ substrates above about 600°C [5]. Under these conditions the observed resistance values should result from a parallel combination of both the film and substrate resistances.

#### 4.2. Substrate properties

Figure 7 shows the resistance behaviour of a bare substrate undergoing a temperature cycle similar to that used during an YBaCuO film elaboration, however under vacuum ( $< 10^{-6}$  torr) in this case. Two salient features appear in the graph: i) An exponential decrease of the resistance with increasing temperature, in line with thermally activated diffusion processes in YSZ; ii) resistance discontinuities through the whole cycle, which may be interpreted by percolation paths building up during heating and destroyed during cooling down.

In fact, we observe charge carrier diffusion rates in good agreement with literature, according to the relationship  $R = R_{\infty} \exp(T_0/T)$ . In the heating up phase, we find  $T_0 \approx 7K$  in fair agreement with  $O^{2-}$  ion diffusion data found in the  $T_0 = 6$  to  $11K$  range for YSZ containing yttria concentrations similar to ours [11]. For the cooling down phase, we find  $T_0 \approx 2.7K$  (to be compared with  $1.4K$  in [12]) for high temperatures, and  $T_0 \approx 0.4K$  (to be compared with  $0.25K$  in [12]) for lower temperatures, in line with hole conductivity resulting from oxygen vacancies created by the vacuum treatment.

These results yield a reasonable qualitative interpretation of the observed resistance variations shown in Fig. 6. It is important to note that, according to the sharp rise of the substrate resistance displayed in figure 7

for the cooling down phase, the resistance variation observed during the major part of the cooling down of an YBaCuO film (of reasonable quality) is dominantly determined by the behaviour of the film undergoing the oxygenation process. This conclusion confirms the validity of the resistance monitoring technique for optimization of the oxygenation parameters.

## 5. Conclusion

A main result concerning the *ex situ* technique is the film resistivity behaviour during the annealing cycle. A sharp resistance drop can be related to a solid-liquid transformation during the high temperature dwell, and a subsequent rise when oxygen is introduced may be linked with a liquid-solid transformation while the tetragonal phase nucleates from the melt.

In addition, we have shown that the resistance monitoring technique remains a valuable tool to characterize the film behaviour during the *in situ* elaboration, even if the resistance variation is influenced by ionic conduction processes occurring in the substrate at high temperatures.

## References

- 1 F. Hosseini Teherani, E. Caristan, F. Carrié, T. Pech, J. Baixeras, A. Kreisler, Proc. ICAM 91, Strasbourg, L. Corra Ed., North Holland (1992) 807.
- 2 J. Baixeras, F. Carrié, F. Hosseini Teherani, A. Kreisler, T. Pech, G. Poulain, J.F. Hamet, J. Muniesa, M. Rapeaux, J. Aymami, SPIE Vol. 1287, C.-C. Chi & R.B. van Dover Eds. (1990) 104.
- 3 A. Kreisler, F. Hosseini Teherani, J.M. Depond, J. Baixeras, M. Redon, G. Alquié, SPIE Vol. 1576, M.R. Siegrist, M.Q. & T.M. Tran Eds. (1991) 636.
- 4 F. Hosseini Teherani, A. Kreisler, J. Baixeras, Proc. SPIE Conf. Vol. 1362, M. Razeghi Ed. (1991) 921.
- 5 Y. Ikuma, K. Komatsu, W. Komatsu, Advances in Ceramics, Vol. 24: Science and Technology of Zirconia III, The American Ceramics Society (1988) 749.
- 6 J.M. Depond, J.C. Martin, F. Carrié, E. Caristan, A. Kreisler, C. Martin, D. Tétard, this Volume.
- 7 T.B. Lindemer, F.A. Washburn, C.S. Mc Dougall, R. Feenstra, O.B. Cavin, Physica C 178 (1991) 93.
- 8 D. Dubreuil, G. Garry, Y. Lemaître, L. Rogier, D. Dieumegard, J. Less-Comm. Metals, 151 (1989) 303.
- 9 J.E. Ullman, R.W. Mc Callum, J.D. Verhoeven, J. Mater. Res. 4 (1989) 752.
- 10 K. Yamamoto, B.M. Lairson, C.B. Eom, R.H. Hammond, J.C. Bravman, T.H. Geballe, Appl. Phys. Lett. 57 (1990) 1936.
- 11 E.C. Subbaro, Advances in Ceramics, Vol. 3, A. Heuer & L.W. Hobbs eds.: Science and Technology of Zirconia I, The American Ceramics Society (1981) 1.
- 12 M. Kleitz, M. Levy, J. Foulletier, P. Fabry, Advances in Ceramics, Vol. 3, Science and Technology of Zirconia I, The American Ceramics Soc. (1981) 337.